Electronic Transduction of DNA Sensing Processes on Surfaces: Amplification of DNA Detection and Analysis of Single-Base Mismatches by Tagged Liposomes

Fernando Patolsky, Amir Lichtenstein, and Itamar Willner*

Contribution from the Institute of Chemistry, The Hebrew University of Jerusalem, Jerusalem 91904, Israel

Received October 9, 2000

Abstract: Tagged, negatively charged, liposomes are used to amplify DNA sensing processes. The analyses of the target DNA are transduced electrochemically by using Faradaic impedance spectroscopy, or by microgravimetric measurements with Au-quartz crystals. By one method, a probe oligonucleotide (**1**) is assembled on Au-electrodes or Au-quartz crystals. The formation of the double-stranded assembly with the analyte DNA (**2**) is amplified by the association of the **3**-oligonucleotide-functionalized liposomes to the sensing interface. The target DNA is analyzed by this method with a sensitivity limit that corresponds to 1×10^{-12} M. A second method to amplify the sensing of the analyte involves the interaction of the **1**-functionalized electrode or Au-quartz crystal with the target DNA sample (**2**) that is pretreated with the biotinylated oligonucleotide (**4**). The formation of the three-component double-stranded assembly between **1**/**2**/**4** is amplified by the association of avidin and biotin-labeled liposomes to the sensing interfaces. By the secondary association of avidin and biotin-tagged liposomes, a dendritic-type amplification of the analysis of the DNA is accomplished. The analyte DNA (**2**) is sensed by this method with a sensitivity limit corresponding to 1×10^{-13} M. The biotin-tagged liposomes are also used to probe and amplify single-base mismatches in an analyte DNA. The **6**-oligonucleotide-functionalized Au-electrode or Au-quartz crystal was used to differentiate the single-base mismatch (G) in the mutant (**5**) from the normal A-containing gene (**5a**). Polymerase-induced coupling of the biotinylated-C-base to the double-stranded assembly generated between **6** and **5** followed by the association of avidin and biotin-tagged liposomes is used to probe the single base mismatch. The functionalized liposomes provide a particulate building unit for the dendritic amplification of DNA sensing.

The development of DNA sensors has attracted recent research efforts directed at gene analysis, the detection of genetic disorders, tissue matching, and forensic applications.[1,2] Optical detection of DNA was accomplished by the use of fluorescence-labeled oligonucleotides[3] or by the application of surface plasmon resonance (SPR) spectroscopy.[4] Fluorescence-based DNA biochip arrays are commercially available.[5] Electronic transduction of oligonucleotide-DNA recognition events, and specifically the quantitative assay of DNA, represent major challenges in DNA bioelectronics.[6] Electrochemical DNA sensors based on the amperometric transduction of the formation of double-stranded oligonucleotide-DNA assemblies in the presence of conducting polymers have been reported. Direct electrochemical assay of double-stranded DNA was previously discussed, but this method reveals[7] low sensitivity and selectivity. Electrostatic attraction of redox-active transition metal complexes,[8] or electroactive dyes[9] to double-stranded (ds) oligonucleotide-DNA or the intercalation of redox-labeled intercalators[10] to ds-DNA, was used for the voltammetric probing of DNA recognition processes.

Two fundamental issues that need to be addressed in the development of DNA sensors relate to the specificity and selectivity of the devices. Amplified DNA analyses using microgravimetric, quartz-crystal-microbalance transduction were reported in the presence of specific antibodies[11] or labeled proteins.[12] Oligonucleotide-functionalized redox enzymes were

* Author to whom correspondence should be addressed.

(1) (a) Mikkelsen, S. R. *Electroanalysis* **1996**, *8*, 15−19. (b) Wilson, E. K. *Chem. Eng. News* **1998**, *76* (21), 47−49.

(2) (a) Millan, K. M.; Mikkelsen, S. R. *Anal. Chem*. **1993**, *65*, 2317−2323. (b) Yang, M. S.; McGovern, M. E.; Thompson, M. *Anal. Chim. Acta* **1997**, *346*, 259−275.

(3) (a) Piunno, P. A. E.; Krull, U. J.; Hudson, R. H. E.; Damha, M. J.; Cohen, H. *Anal. Chim. Acta* **1994**, *288*, 205−214. (b) Nilsson, M.; Krejci, K.; Kwiatkowski, M.; Gustavsson, P.; Landergen, U. *Nat. Genet*. **1997**, *16*, 252−255.

(4) (a) Lidberg, B.; Nylander, C.; Lundström, I. *Sens. Actuators* **1983**, *4*, 299−302. (b) Jordan, C. E.; Frutos, A. G.; Thiel, A. J.; Corn, R. M. *Anal. Chem*. **1997**, *69*, 4939−4947.

(5) (a) Ekins, R.; Chu, F. W. *Trends Biotechnol*. **1999**, *17*, 217−218. (b) Pinkel, D.; Seagraves, R.; Sudar, D.; Clark, S.; Poole, I.; Kowbel, D.; Collins, C.; Kuo, W. L.; Chen, C.; Zhai, Y.; Dairkee, S. H.; Ljung, B. M.; Gray, J. W.; Albertson, D. G. *Nat. Genet.* **1998**, *20*, 207−211. (c) Pease, A. C.; Solas, D.; Sullivan, E. J.; Cronin, M. T.; Holmes, C. P.; Fodor, S. P. A. *Proc. Natl. Acad. Sci. U.S.A.* **1994**, *91*, 5022−5026. (d) Livache, T.; Fouque, B.; Roget, A.; Marchand, J.; Bidan, G.; Teoule, R.; Mathis, G. *Anal. Biochem*. **1998**, *255*, 188−194. (e) Arlinghaus, H. F.; Kwoka, M. N.; Jacobson, K. B. *Anal. Chem*. **1997**, *69*, 3747−3753.

(6) (a) Wang, J.; Palecek, E.; Nielsen, P. E.; Rivas, G.; Cai, X. H.; Shiraishi, H.; Dontha, N.; Luo, D. B.; Farias, P. A. M. *J. Am. Chem. Soc*. **1996**, *118*, 7667−7670. (b) Ihara, T.; Nakayama, M.; Murata, M.; Nakano, K.; Maeda, M. *Chem. Commun*. **1997**, 1609−1610.

(7) Korri Youssoufi, H.; Garnier, F.; Srivastava, P.; Godillot, P.; Yassar, A. *J. Am. Chem. Soc.* **1997**, *119*, 7388−7389.

(8) Millan, K. M.; Saraullo, A.; Mikkelsen, S. R. *Anal. Chem*. **1994**, *66*, 2943−2948.

(9) Hashimoto, K.; Ito, K.; Ishimori, Y. *Anal. Chem*. **1994**, *66*, 3830−3833.

(10) Takenaka, S.; Yamashita, K.; Takagi, M.; Uto, Y.; Kondo, H. *Anal. Chem*. **2000**, *72*, 1334−1341.

(11) Bardea, A.; Dagan, A.; Ben-Dov, I.; Amit, B.; Willner, I. *Chem. Commun*. **1998**, 839−840.

(12) Bardea, A.; Patolsky, F.; Dagan, A.; Willner, I. *Chem. Commun*. **1999**, 21−22.

10.1021/ja0036256 CCC: $20.00
Published on Web 05/11/2001

used to probe the formation of oligonucleotide-DNA ds-assemblies by the electrical contacting of the redox -enzyme with the electrode, and the activation of a secondary bioelectrocatalytic transformation.[13] The amplified DNA sensing was reported by coupling to the double-stranded DNA assembly associated with the electronic transducer an oligonucleotide-enzyme conjugate that precipitates an insoluble product on the transducer. The biocatalyzed precipitation of the insoluble product on an electrode or a piezoelectric quartz crystal provides an amplification route for the primary DNA recognition event.[14] Faradaic impedance spectroscopy and microgravimetric quartz-crystal-microbalance measurements were used as transduction methods for the amplified sensing processes. Recently, oligonucleotide-functionalized Au nanoparticles were used for a dendritic-type amplification route of DNA sensing, and the microgravimetric, quartz-crystal-microbalance measurements were used as the electronic transduction means of the analytical process.[15] Enzyme labels integrated with biotinylated liposomes, acting as carriers, were used as biocatalytic amplifiers in DNA detection schemes.[16] We recently reported on the use of oligonucleotide-functionalized liposomes or biotin-labeled liposomes as labels for the dendritic amplification of DNA sensing events.[17] The liposomes that bind to the generated oligonucleotide-DNA assembly alter the interfacial properties of electronic transducers such as electrodes or Au/quartz crystals, thus enabling the electrochemical or microgravimetric transduction of the amplified sensing processes. The specific sensing of DNA was addressed by controlling the temperature during hybridization with the analyte or mutant DNAs.[18] Nonetheless, this method assumes identical concentrations of the mutants and the DNA, and is of limited applicability at variable concentrations of the different DNAs. We have suggested[16,17] the use of a 12-mer oligonucleotide as a specific sensing interface that is complementary to the target DNA. This oligonucleotide forms a full, and single, ds-turn with the analyte DNA, and any base mismatch substantially perturbs the thermodynamic helix stability. This enabled the specific detection of the analyte DNA at an impressive concentration difference between the analyte and the mutant.

In the present study we describe the detailed and comprehensive results on the use of tagged liposomes as probes for the amplification of DNA sensing processes. In contrast to previous studies that use liposomes as carriers for a biocatalytic amplifying agent,[16] the present study highlights the use of liposomes as a particulate building unit for the dendritic amplification of DNA sensing. We address the detailed characterization of the oligonucleotide sensing interface and the quantitative analysis of the DNA by different techniques including chronocoulometry, Faradaic impedance spectroscopy, and quartz-crystal microbalance measurements. We reveal unprecedented sensitive and specific detection of DNA. Finally, we use the tagged liposomes as labels for the detection of single-base mismatches in DNA.

(13) (a) de Lumley Woodyear, T.; Campbell, C. N.; Heller, A. *J. Am. Chem. Soc*. **1996**, *118*, 5504−5505. (b) Caruana, D. J.; Heller, A. *J. Am. Chem. Soc*. **1999**, *121*, 769−774.

(14) Patolsky, F.; Katz, E.; Bardea, A.; Willner, I. *Langmuir* **1999**, *15*, 3703−3706.

(15) Patolsky, F.; Ranjit, K. T.; Lichtenstein, A.; Willner, I. *Chem. Commun*. **2000**, 1025−1026.

(16) Alfonta, L.; Singh, A. K.; Willner, I. *Anal. Chem.* **2001**, *73*, 91−102.

(17) (a) Patolsky, F.; Lichtenstein, A.; Willner, I. *Angew. Chem., Int. Ed*. **2000**, *39*, 940−943. (b) Patolsky, F.; Lichtenstein, A.; Willner, I. *J. Am. Chem. Soc*. **2000**, *122*, 418−419.

(18) Okahata, Y.; Kawase, M.; Niikura, K.; Ohtake, F.; Furusawa, H.; Ebara, Y. *Anal. Chem*. **1998**, *70*, 1288−1296.

Experimental Section

Materials. Phosphatidic acid(1,2-diacyl-*sn*-glycerol-3-phosphate), phosphatidyl choline (1-hexadecanoyl-2-[*cis*-9-octadecanoyl]-*sn*-glycero-phosphocholine) EDTA, Avidin-alkaline phosphatase, 5-bromo-4-chloro-3-indolyl phosphate, dithiotreitol, calf thymus DNA, Biotin-dCTP, and Polymerase I (Klenow fragment) were all purchased from Sigma. Maleimide phosphatidylethanolamine *N*-((4-maleimidemethyl)-cyclohexane- 1-carbonyl)-1,2-dihexadecanoyl-1-phosphatydilethanolamine), biotin-x-DHPE(*N*-(biotinoyl)-1,2-dihexadecanoyl-*sn*-glycero-3-phosphoethanolamine), PicoGreen (dsDNA quantitation reagent), and OliGreen (ssDNA quantitation reagent) were purchased from Molecular Probes Inc; oligonucleotides of appropriate sequences and labels were custom ordered from Genset.SINGAPORE Biotech. ^{3}H-Cholesterol (45 Ci/mol) and NAP-10 columns of Sephadex G-25 were purchased from Amersham Pharmacia.

Instruments. A potentiostat/Galvanostat (EG&G model 283) and Impedance Analyzer (EG&G model 1025) connected to a personal computer (EG&G Software Power suite 1.03 and #270/250 for Impedance and chronopotentiometry measurements, respetively) were used for the electrochemical measurements. A home-built QCM analyzer equipped with a Fluke 164'T' multifunction counter was used for the microgravimetric quartz-crystal-microbalance experiments. A fluorimeter (Perkin-Elmer 540), a sonicator-(Sonicator W-385, Ultrasonics USA), an ultracentrifuge (Optima ultracentrifuge, Beckman), and a scintillation counter (6000TA, Beckman) were used for the preparation and the characterization of the liposomes. Dynamic Light Scattering experiments were performed with a Zetasizer 3000 (Malvern Instruments).

Methods. (a) Electrode Characterization and Pretreatment. Gold wire electrodes (0.5 mm diameter, ca. 0.2 cm^2 geometrical area, roughness factor, ca. 1.2−1.5) were used for the electrochemical measurements. To remove any previous organic layer, and to generate the bare metal surface, the electrodes were cleaned by using super saturated hot KOH solution for 2 h, and then treated for 15 min with a pyranha solution (70% H_2SO_4:30% H_2O_2). WARNING: PIRANHA SOLUTION REACTS VIOLENTLY WITH ORGANIC SOLVENTS. The resulting electrodes were further cleaned by electrochemical sweeping in 1 M H_2SO_4 from 0 to −1.5 V.

(b) Electrochemical Measurement. A conventional three-electrode cell, consisting of the modified-Au electrode as working electrode, a glassy carbon auxiliary electrode isolated by a glass frit, and a saturated calomel electrode (SCE) connected to the working volume with a Luggin capillary, was used for the electrochemical measurements. The cell was positioned in a grounded Faradaic cage. All electrochemical measurements were performed in 100 mM phosphate buffer at pH 7.5 as a background electrolyte solution, unless otherwise stated.

Chronocoloumetry experiments were performed in an electrolyte solution that included 50 μM $Ru(NH_3)_6^{+3}$ in 10 mM Tris buffer at pH 7.5. Faradaic impedance measurements were performed in an electrolyte solution composed of a 5 mM $K_3[Fe(CN)_6]$/ $K_4[Fe(CN)_6]$ 1:1 mixture in 100 mM phosphate buffer, pH 7.2. Impedance measurements were performed at a bias potential of 0.18 V vs SCE, using an alternating voltage of 5 mV, in the frequency range of 100 MHz to 20 kHz. The impedance spectrum was plotted in the form of the complex plane diagrams (Nyquist plots).

(c) Quartz-Crystal Microbalance Measurements. Quartz crystals (AT-cut, 9 MHz) sandwiched between two Au electrodes (roughness factor ca. 3.5 with an area of 0.196 cm^2, Seiko) were used in microgravimetric experiments. Quartz electrodes were cleaned with a pyranha solution (70% H_2SO_4:30% H_2O_2) for 15 min, then rinsed thoroughly with double deionized water and dried with a stream of argon.

(d) Preparation of Thiolated Oligonucleotides. The thiolated oligonucleotides were freshly reduced prior to the modification of the electrodes or the preparation of oligonucleotide-tagged liposomes. The alkanethiol-functionalized oligonucleotides have the following sequences: (**1**) 5′-TCT ATC CTA CGC T-$(CH_2)_6$-SH-3′, (**3**) 5′-HS-$(CH_2)_6$-GCG CGA ACC GTA TA-3′, and (**6**) 5′-HS-(CH_2)-CGT TTG ATT ACT GGC CTT GCG GATC-3′ were commercially prepared as the respective disulfides.

(**1**) or (**3**) or (**6**) disulfides, ca. 20 O.D. each, were dissolved in PBS buffer (137 mM NaCl, 2.8 mM KCl, 8.1 mM Na_2HPO_4, 1.5 mM KH_2PO_4, pH 7.5). All oligonucleotides were reduced in the presence of 0.04 M DTT. The respective mixture was allowed to react for 16 h at room temperature and the resulting solution was eluted through a NAP-10 column of Sephadex G-25. The thiolated oligonucleotide concentration after elution was ca. 90 μM. Prior to their use the oligonucleotides were diluted to the required concentration with a PBS/EDTA solution, pH 7.5 (137 mM NaCl, 2.8 mM KCl, 8.1 mM Na_2HPO_4, 1.5 mM KH_2PO_4, 10 mM EDTA).

(e) Preparation of Anionic Liposomes. Large unilamellar anionic vesicles (LUV) were prepared by modification of the literature method.[19,20] The vesicles were composed of phosphatidic acid• phosphatidyl choline, maleimide-phosphatidylethanolamine, and ^{3}H-Cholesterol in the molar ratio of 79:20:1:0.1, final lipid concentration 5 mM. The lipids were used without further purification. Dynamic light scattering was used to determine the vesicle size using an argon ion laser at 488 nm. The refractive index of the LUV particles was assumed[21] to be 1.49. The radius of the vesicle was calculated from the correlation function and was established to be unimodal with a diameter in the range of 220 ± 20 nm. The LUV concentration was determined by measuring the radioactivity of the vesicles.

(f) Preparation of DNA-Tagged Anionic Liposomes. Anionic large Unilamellar Vesicles Liposomes (LUV) (2.5 mM) and oligonucleotide **3** (final concentration of 29 μM in 0.15 M PBS + 10 mM EDTA, pH 7.5) were reacted overnight at 4 °C. The DNA-tagged liposomes were purified by column chromatography (Sephadex G-75). Eight fractions, 0.4 mL each, were collected. For each fraction, the DNA surface coverage and lipid concentration were determined. The surface coverage of **3** on the liposomes was estimated by following the fluorescence intensity of the OliGreen dye that was associated with it, whereas the liposome concentration was determined by measuring its radioactivity.

(g) Preparation of Biotin-Labeled Liposomes. LUV biotinylated liposomes were composed of phosphatidyl choline (1-hexadecanoyl-2-[*cis*-9-octadecanoyl]-*sn*-glycero-3-phosphocholine), phosphatidylethanolamine (1,2-dihexadecanoyl-*sn*-glycero-3-phosphoethanolamine), biotin-x-DHPE(*N*-(biotinoyl)-1,2-dihexadecanoyl-*sn*-glycero-3-phosphoethanolamine), and ^{3}H-Cholesterol (45 Ci/mol) in the molar ratio of 80:20:0.1:0.1.

The lipid ingredients were solubilized in a mixture of chloroform: methanol 10:1 (v/v) and the solution was rotary evaporated under reduced pressure in a round-bottomed flask to create a phospholipid film. The lipid film was dispersed by vortexing it with PBS at pH 7.5. The lipid dispersion was incubated in a water bath at 40 °C for 2 h. The resulting suspension was further sonicated and centrifuged by using an identical procedure to that described for the preparation of the anionic LUV.

The liposome concentration was determined by radioactivity measurements to be 2.5 mM. The liposomes were further purified by affinity chromatography (DEAE Sephadex A-25). The working fraction had a concentration of 1.4 mM. The hydrodynamic diameter of the biotin-LUV was determined by dynamic light scattering to be unimodal with a diameter of 180 ± 40 nm.

(h) Modification of Au Electrodes with Oligonucleotides. DNA-modified gold electrodes or Au/quartz crystals were prepared by incubating the clean electrodes or quartz crystals with the thiolated oligonucleotide. For the detection of the target DNA (**2**) by the process outlined in Scheme 1A, clean gold electrodes or Au/quartz crystals were incubated in PBS buffer solution (0.2 M, pH 7.5), containing the thiolated oligonucleotide (**1**) at a concentration of ca. 5 μM, at room temperature, for 90 min, unless otherwise stated. For the detection of the single-base mutation, the clean gold electrodes or Au/quartz crystals were incubated in a buffer solution (PBS buffer, 0.16 M, pH 7.4) containing the thiolated primer (**6**), at a concentration of ca. 5 μM at room temperature for a period of 90 min, unless otherwise stated. After the primer modification was completed the electrodes were rinsed thoroughly with PBS buffer, pH 7.5, and finally with deionized water.

(i) DNA Hybridization. For the process outlined in Scheme 1A, the **1**-modified gold electrodes were incubated at 37 °C in a buffer solution (2 × SSC buffer, pH 7.5) containing the target DNA (**2**) at different concentrations and for the specified time intervals. For the detection of single-base mismatches, as outlined in Scheme 2, the **6**-functionalized electrodes or Au/quartz crystals were incubated in a 2 × SSC buffer solution, pH 7.5, containing the target DNA (**5** or **5a**) at different concentrations, for a period of 60 min.

(j) Detection of Single-Base Mismatch. The **6**-functionalized electrodes were reacted either with the complementary ssDNA that carried the mutation (**5**) or the normal sequence (**5a**). Biotinylated dCTP (20 μM) was incorporated by the action of polymerase Klenow fragment 20 U/mL in Tris buffer solution (20 mM Tris HCl, $MgCl_2$ 10 mM, KCl 60 mM), pH 7.5.

The biotinylated assembly was further reacted with avidin, 2.5 μg/mL, in 0.1 M Tris-buffer solution, pH 7.5 for 15 min, and then reacted with the biotin-labeled liposomes (lipid concentration 0.25 mM) for 20 min.

Results and Discussion

The methods for the amplified detection of an analyte DNA are schematically depicted in Scheme 1. By one method, Scheme 1A, a probe oligonucleotide (**1**), complementary to the target analyte DNA (**2**), is assembled on the transducer. In the presence of the analyte (**2**), a double-stranded assembly is formed on the surface. The resulting assembly is then interacted with the **3**-oligonucleotide-functionalized liposome. The latter oligonucleotide is complementary to the other end of the single-stranded target DNA, and thus a three-component double-stranded (ds) assembly functionalized by the liposomes is formed on the transducer. The association of the liposomes onto transducers such as electrodes or piezoelectric crystals alters the properties of the interfaces of the conductive supports or the mass associated with piezoelectric crystals, and thus Faradaic impedance spectroscopy[22] or quartz-crystal-microbalance measurements[23] could act as electronic transduction means for the DNA sensing events (vide infra). The second method for the amplified sensing of DNA is displayed in Scheme 1B. The primer (**1**) is assembled as the sensing interface on the transducer. The sample that includes the analyte is pretreated with the biotinylated oligonucleotide (**4**) that is complementary to one end of the target oligonucleotide. Interaction of the sensing interface with the double-stranded complex between **2** and **4** yields a biotin-labeled three-component ds assembly. Further treatment of the surface with avidin and then with the biotin-tagged liposome results in the association of the liposome to the interface. By the subsequent treatment of the interface with avidin and then with the biotin-labeled liposomes, a second generation of biotin-labeled liposomes is linked to the assembly. Note that a single sensing event yields, in the second step of interaction with the liposomes, a dendritic-type structure and amplification. The association of the liposomes to the sensing interface changes the interfacial properties of an electrode, or the mass associated with a piezoelectric crystal on which the primer is assembled, respectively, and thus Faradaic impedance spectroscopy, or microgravimetric quartz crystal microbalance

(19) Hauser, H.; Gains, N.; Muller, M. *Biochemistry* **1983**, *22*, 4775−4781.

(20) Aurora, S. T.; Wei, L.; Cummins, Z. H.; Haines, H. T. *Biochim. Biophys. Acta* **1985**, *820*, 250−258.

(21) Chong, C. S.; Colbow, K. *Biochim. Biophys. Acta* **1976**, *436*, 260−282.

(22) (a) Bard, A. J.; Faulkner, L. R. *Electrochemical Methods; Fundamentals and Applications*; Wiley: New York, 1980. (b) Stoynov, Z. B.; Grafov, B. M.; Savova-Stoynov, B. S.; Elkin, V. V. *Electrochemical Impedance*; Nauka: Moscow, 1991.

(23) (a) Buttry, D. A. In *Eletroanalytical Chemistry*; Bard, A. J., Ed.; Marcel Dekker: New York, 1991; Vol. 17, pp 1−82. (b) Lu, C.; Czanderna, A. W., Eds. *Applications of Piezoelectric Quartz Crystal Microbalances, Methods and Phenomena*; Elsevier Science Publishing: New York, 1984; Vol. 7.

Scheme 1. (A) The Amplified Sensing of a Target DNA with Oligonucleotide-Functionalized Liposomes[a] and (B) Sensing of a Target DNA with a Biotinylated Oligonucleotide, Avidin and Liposomes Labeled with Biotin as an Amplification Conjugate[b]

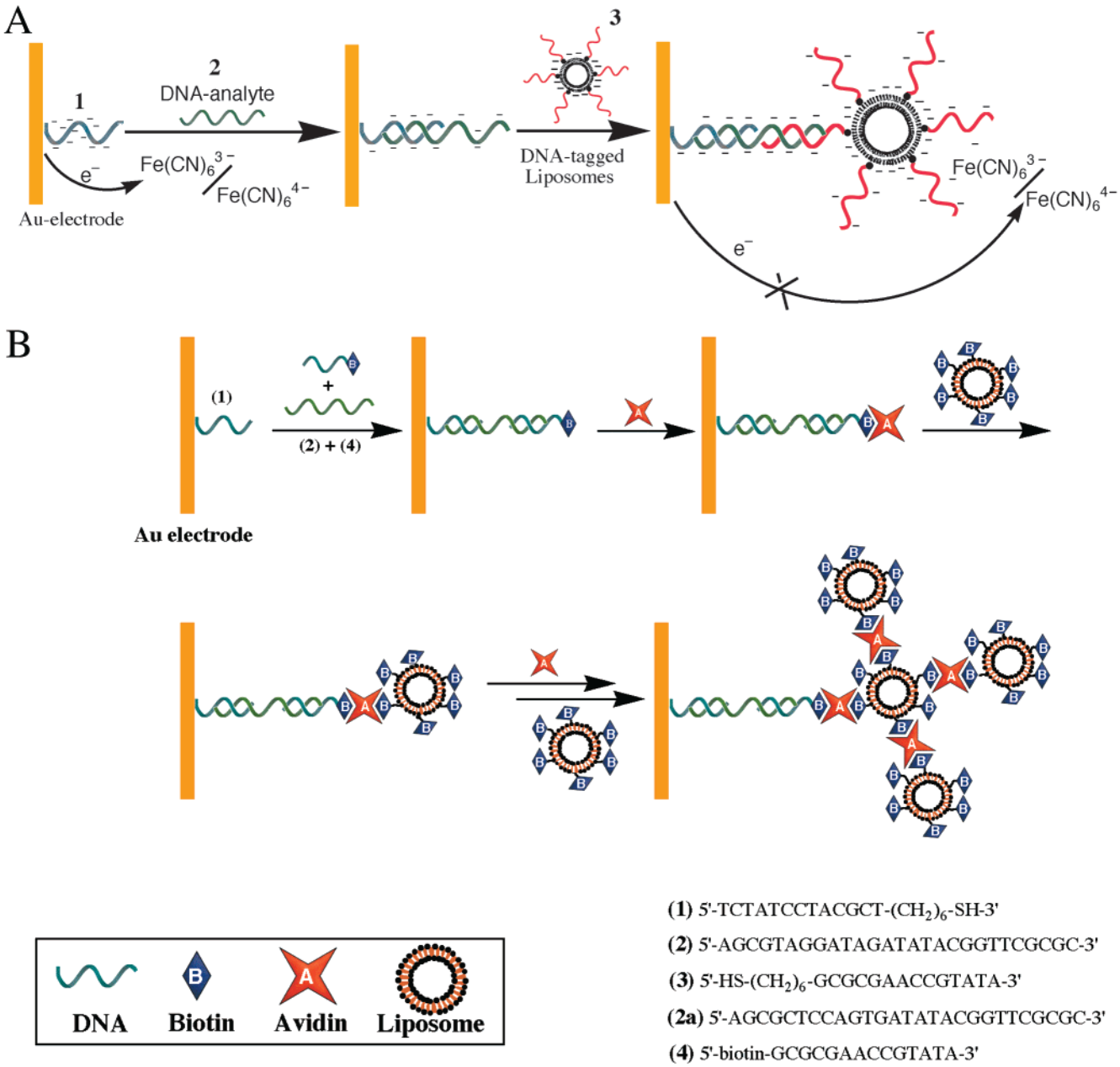

[a] Oligonucleotides **1**, **2**, and **3** are represented by blue, green, and red wavy curves, respectively. [b] Green wavy lines indicate oligonucleotide **2**, blue wavy curves correspond to oligonucleotide **4**, blue diamonds correspond to biotin, red stars represent avidin.

measurements, could be employed to transduce the sensing process (vide infra).

The preparation of the liposomes and the methods used for their structural analysis are detailed in the Experimental Section. Liposomes consisting of phosphatidic acid, phosphatidyl choline, maleimide phosphatidyl ethanolamine (*N*-(4-maleimidemethyl)-cyclohexane-1-carbonyl)-1,2-dihexadecanoyl-1-phosphatidyl ethanolamine), and ^{3}H-cholesterol at a molar ratio that corresponds to 79:20:1:0.1 were prepared. The radioactive cholesterol marker is introduced into the liposomes to enable the rapid determination of the concentration of the liposomes. The liposomes were reacted with the oligonucleotide (**3**) to yield the **3**-functionalized liposomes. The average surface coverage of the liposomes by **3** was estimated to be 50−60 oligonucleotide units per liposome by following the fluorescence intensity of the purified liposomes in the presence of OliGreen that binds to the single-stranded DNA. Dynamic light scattering experiments revealed that the liposomes had a diameter of 220 ± 20 nm. The biotin-labeled liposomes consist of a mixture of phosphatidyl choline (2-hexadecanoyl-2-[*cis*-9-octadecanoyl]-*sn*-glycero-3-phosphocholine), phosphatidyl-ethanolamine (1,2-dihexadecanoyl-*sn*-glycero-3- phosphoethanolamine), ^{3}H-cholesterol, and *N*-(biotinyol)-1,2-dihexadecanoyl-*sn*-glycero-3-phosphoethanolamine at a ratio of 80:20:0,1:0,1, respectively. The size of the liposomes was determined by dynamic light scattering experiments to have a diameter of 180 ± 40 nm. The two kinds of labeled liposomes are negatively charged. This electrical negative charge of the liposomes is pre-designed to prevent the nonspecific binding of the liposomes to the oligonucleotide interface, Scheme 1A,B. The association of a liposome to a double-stranded oligonucleotide-DNA assembly leads to the formation of a charged micromembrane interface on the transducer as a result of the primary recognition event of the analyte DNA. Thus, the binding of the liposomes to the sensing

Scheme 2. Electronic Transduction of a Single Base Mutation in the Target-DNA, (**5**), with Polymerase-Induced Coupling of a Biotinylated-Base and Biotin-Labeled Liposomes as an Amplification Route

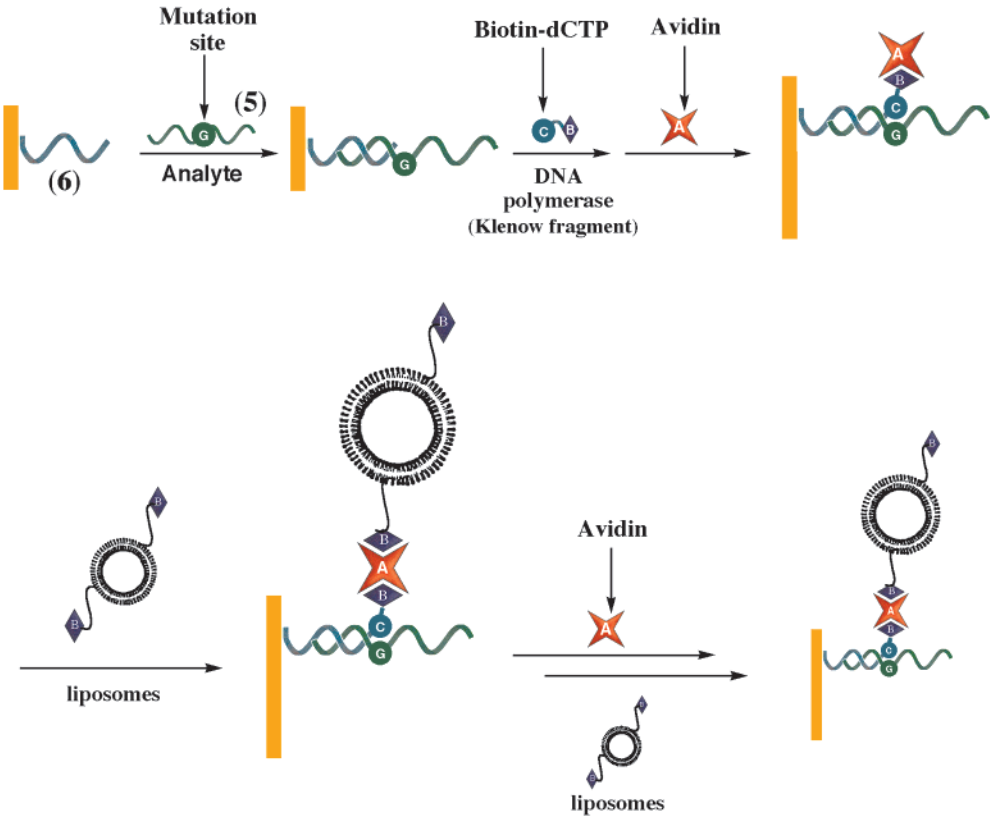

(5) 5' - CTT TTC TTT TCT TTT **G**GA TCC GCA AGG CCA GTA ATC AAA CG - 3'

(5a) 5' - CTT TTC TTT TCT TTT **A**GA TCC GCA AGG CCA GTA ATC AAA CG - 3

(6) 5' - HS-$(CH_2)_6$ - CGT TTG ATT ACT GGC CTT GCG GAT C - 3'

interface is anticipated to alter the interfacial properties of the transducer. In the presence of a negatively charged redox label, e.g. $Fe(CN)_6^{3-}/Fe(CN)_6^{4-}$, the interfacial electron transfer should be hindered as a result of the electrostatic repulsion of the redox label by the liposome interface. Faradaic impedance spectroscopy would be an effective method to probe the interfacial electron-transfer resistance at the functionalized electrode.[22]

The complex impedance can be presented as the sum of the real components, $Z_{re}(\omega)$, that originate mainly from the resistance and capacitance of the cell. The general electronic equivalent scheme (Randles and Ershler model)[24] includes the ohmic resistance of the electrolyte solution, R_s, the Warburg impedance, Z_w, resulting from the diffusion of ions from the bulk electrolyte to the electrode interface, the double layer capacitance, C_{dl}, and the electron-transfer resistance, R_{et}, that exists if a redox probe is present in the electrolyte solution. The two components of the electronic scheme, R_s and Z_w, represent bulk properties of the electrolyte solution and diffusion features of the redox probe in solution. Therefore, these parameters are not affected by chemical transformations occurring at the electrode surface. The other two components in the scheme, C_{dl} and R_{et}, depend on the dielectric and insulating features at the electrode/electrolyte interface. Indeed, Faradaic impedance spectroscopy was reported[25] as a sensitive method to probe the functionalization of electrodes with proteins and to follow the formation of insulating layers on electrode supports. A typical shape of a Faradaic impedance spectrum (presented in the form of a Nyquist plot) includes a semicircle region lying on the Z_{re} axis followed by a straight line. The semicircle portion, observed at higher frequencies, corresponds to the electron-transfer-limited process, whereas the linear part is characteristic of the lower frequencies range and represents the diffusional-limited electron-transfer process. The electron-transfer kinetics and diffusional characteristics can be extracted from the spectra. The semicircle diameter is equal to R_{et}, whereas the intercept of the semicircle with the Z_{re}-axis at high frequencies ($\omega \rightarrow \infty$) is equal to R_s. Extrapolation of the circle to lower frequencies yields an intercept corresponding to $R_s + R_{et}$.

Microgravimetric quartz-crystal-microbalance measurements provide a further method to probe the functionalization of a piezoelectric crystal with the sensing interface. Specifically, the method should enable the detection of the mass changes occurring on the quartz crystal as a result of the association of macromolecular liposome units. The Sauerbrey equation, eq 1, expresses the mass change, Δm, occurring on the crystal with the crystal frequency changes, Δf, where f_o is the frequency of the quartz crystal prior to a mass change, Δm is the mass change, A is the piezoelectrically active area, ρ_q is the density of quartz

(24) (a) Randles, J. *Discuss. Faraday Soc.* **1947**, *1*, 11−20. (b) Ershler, B. V. *Discuss. Faraday Soc.* **1947**, *1*, 269−274.

(25) Patolsky, F.; Zayats, M.; Katz, E.; Willner, I. *Anal. Chem.* **1999**, *71*, 3171−3180.

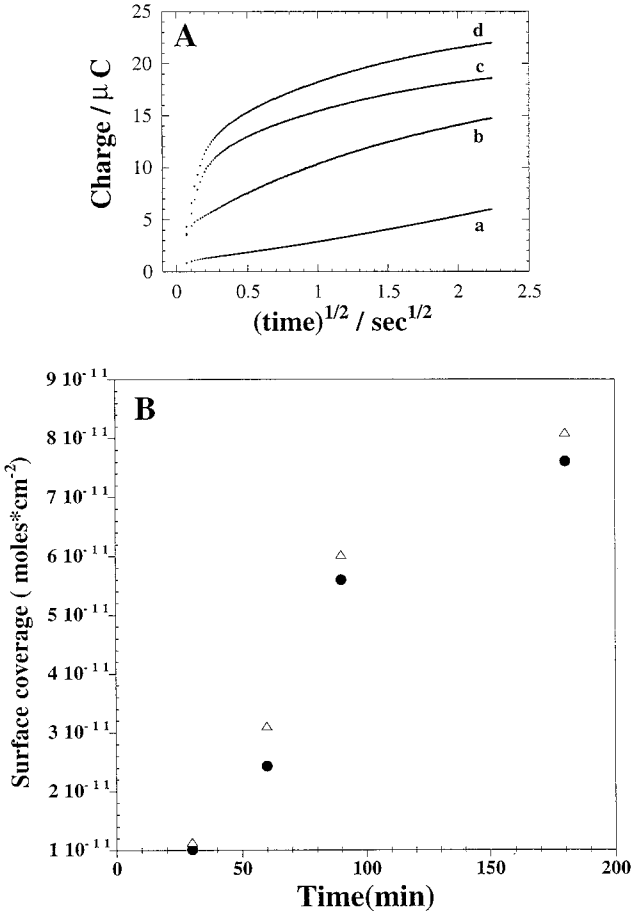

Figure 1. (A) Chronocoulometric transients for (a) a bare Au electrode and (b, c, and d) after modification of the electrode in the presence of **1**, 5 μM, for 60, 90, and 180 min, respectively. (B) Surface coverage of **1** derived by chronocoulometry (△) and by microgravimetric experiments (●), at different time intervals of modification with **1**, 5 μM.

(2.648 g·cm^{-3}), and μ_q is the shear modulus (2.947 × 10^{11} dyn·cm^{-2} for AT-cut quartz). Due to the dimensions of the

$$\Delta f = -2f_o^2 \frac{\Delta m}{A(\mu_q \rho_q)^{1/2}} \qquad (1)$$

liposomes we do not apply the Sauerbrey relation to extract quantitative mass changes that occur on the quartz crystal as a result of the association of the liposomes. We use, however, the frequency changes of the piezoelectric crystal as a qualitative measure that follows the association of proteins or liposomes onto the crystal surface. Also, we use the frequency changes of the piezoelectric crystal for the quantitative analysis of the surface coverage of the DNA monolayers.

An Au electrode was functionalized with the thiol-functionalized oligonucleotide (**1**). Figure 1A shows the chronocoulometric assay of the stepwise modification of the electrode with **1**, according to Tarlov's method.[26] The redox-label $Ru(NH_3)_6^{3+}$ is used to probe the content of the oligonucleotide (**1**) on the conductive support. Figure 1A shows the chronocoulometry transients that correspond to the bare Au electrode, curve a, and the transients upon the modification of the electrode with **1** for different time intervals, curves b−d. As the time of modification is longer, the charge associated with the redox

(26) Steel, A. B.; Herne, T. M.; Tarlov, M. J. *Anal. Chem.* **1998**, *70*, 4670−4677.

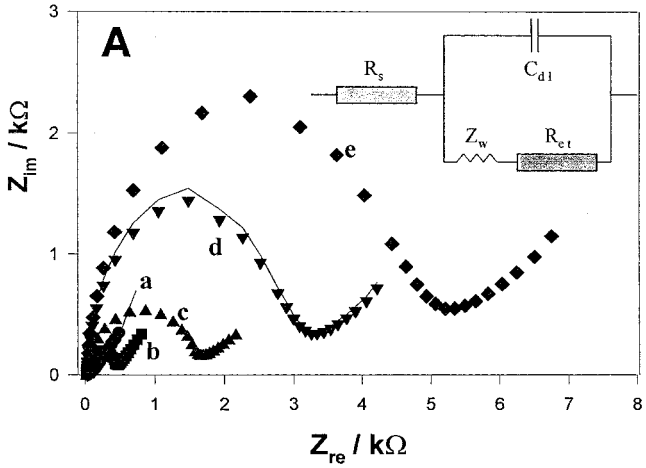

Figure 2. Faradaic impedance spectra of (a) a bare Au electrode and (b, c, d, and e) after modification of the Au electrode with **1**, 5 μM, for 30, 60, 90, and 180 min. The solid line in curve d corresponds to the theoretical fit of the experimental results according to the equivalent circuit shown in the inset. Inset: Equivalent circuit corresponding to the impedance features of the DNA-surface modified electrode.

process of $Ru(NH_3)_6^{3+}$ is higher. The surface coverage of the phosphate units on the electrode is deduced by using eq 2, where

$$Q = \frac{2nFAD_o^{1/2}C_o^*}{\pi^{1/2}} t^{1/2} + Q_{dl} + nFA\Gamma_o \qquad (2)$$

n is the number of electrons per molecule for the reduction of $Ru(NH_3)_6^{3+}$, F is the Faraday constant (C/equiv), A is the electrode area (cm^2), D_o is the diffusion coefficient (cm^2/s), Co* is the bulk concentration of the redox label (mol/cm^2), Q_{dl} is the capacitive charge (C), and $nFA\Gamma_o$ is the charge associated with the reduction of Γ_o (mol/cm^2) of the adsorbed redox marker. The probe surface density Γ_{DNA} (in moles/cm^2) is calculated by using eq 3, where m is the number of bases in the probe

$$\Gamma_{DNA} = \Gamma_o(z/m)(N_A) \qquad (3)$$

DNA, z is the charge of the redox molecule, and N_A is Avogadro's number. The DNA surface coverage on the electrode at different time intervals of modification with **1** was calculated, Figure 1B. The modification of the Au surface with **1** was also followed by microgravimetric quartz-crystal-microbalance measurements. Au-functionalized quartz crystals (9 MHz, AT-cut) were modified with **1**, and the crystal frequency changes were monitored in air at time intervals of modification. The surface coverage of **1** on the Au-quartz crystal was calculated, Figure 1B. We see that the values of the surface coverage of **1** derived by the two methods are very similar and the values determined by chronocoulometry are slightly higher. Figure 2 shows the Faradaic impedance spectra of the electrode upon its functionalization with **1** for different time intervals. We find that the interfacial electron-transfer resistance increases as the modification of the electrode is prolonged. We employ $Fe(CN)_6^{3-}/Fe(CN)_6^{4-}$ as the redox label in solution. Thus, the increase of the interfacial electron transfer resistance upon the modification of the electrode is consistent with the fact that the redox label is electrostatically repelled by the oligonucleotide (**1**) that is associated with the electrode, and the repulsion is

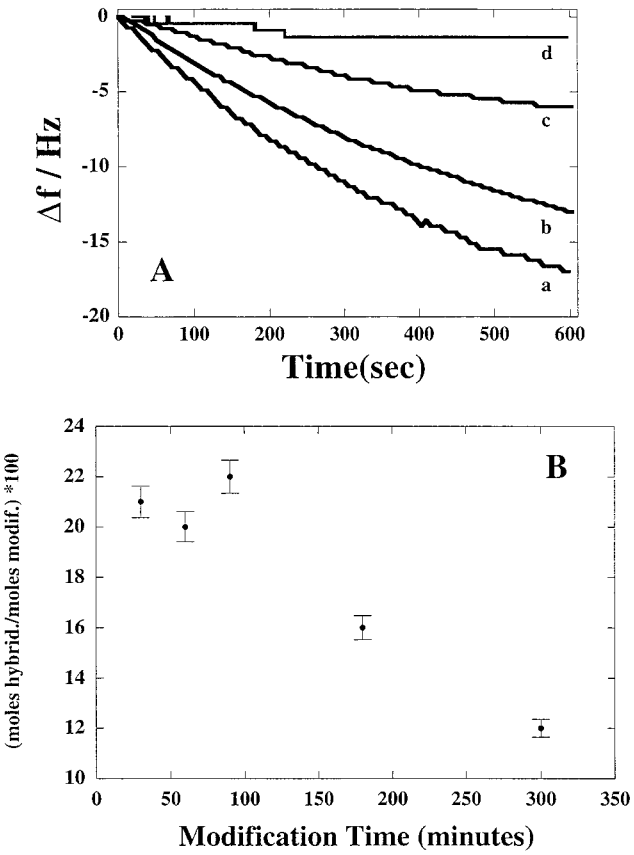

Figure 3. (A) Time-dependent frequency changes of the **1**-modified Au-quartz crystal upon interaction with **2**: (a) 5×10^{-6} M; (b) 5×10^{-7} M; (c) 5×10^{-8} M; and (d) 5×10^{-9} M. Hybridization reactions were performed at 37 °C, in 2 × SSC buffer, pH 7.5. (B) Mole fraction of hybridized DNA (**2**) with the **1**-modified sensing interface generated by the interaction of the Au electrode with **1**, 5×10^{-6} M, for variable time intervals. The hybridization is conducted by the treatment of the sensing interface with **2**, 5×10^{-6} M, in 2 × SSC buffer, pH 7.5, for 10 min.

enhanced as the surface coverage of **1** is higher.[27] The solid line in Figure 2, curve d, corresponds to the theoretical fit of the experimental Faradaic impedance spectrum according to the equivalent circuit outlined in Figure 2 (inset), $R_{et} = 3.3$ kΩ, $C_{dl} = 23\ \mu$F/cm^2. The derived equivalent circuit is identical to the equivalent circuits that were reported for other biomaterial monolayer-functionalized electrodes.[28]

Figure 3A shows the time-dependent frequency changes of the Au-quartz crystal modified with **1** upon the interaction with different concentrations of the analyte DNA (**2**). As the concentration of the target DNA (**2**) in the sample is higher, the decrease of crystal frequencies increases in value, implying that higher amounts of **2** are hybridized with the sensing interface. The amounts of double-stranded oligonucleotide (**1**)/target-DNA (**2**) assemblies that are generated on the sensing interface are affected by the surface coverage of the sensing electrode with the probe oligonucleotide (**1**). Figure 3B shows the mole fraction of hybridized DNA with the sensing interface that is formed upon the interaction of surfaces modified for variable time intervals with **1**, with a constant concentration of **2**, 5×10^{-6} M, for a fixed time interval of 10 min. For example, for the electrode modified with **1** for 90 min, the surface coverage of **1** corresponds to ca. 6×10^{-11} mol·cm^{-2}. After treatment with **2**, 5×10^{-6} M, for 10 min, the mole fraction of ds-oligonucleotide-DNA that is formed on the surface is ca. 22% (surface coverage of ds assemblies is ca. 1.3×10^{-11} mol·cm^{-2}). When the surface is modified with **1** for 300 min, the surface coverage corresponds to ca. 1×10^{-10} mol·cm^{-2}, but after interaction with **2**, the mole fraction of hybridized DNA corresponds only to ca. 12%. (Surface coverage of the ds assembly between **1** and **2** is ca. 1.2×10^{-11} mole·cm^{-2}.) Thus, despite the fact that the surface coverage of the sensing interface increases from 6×10^{-11} to 1×10^{-10} mol·cm^{-2}, by prolonging the modification time of the electrode with **1** from 90 to 300 min, the sensing efficiency of the analyte DNA,by the surface with the high coverage of **1** is not improved. This is explained by steric hindrance to the formation of the ds assembly on the surface with higher coverage of **1**, as well as to enhanced electrostatic repulsion of **2** by the interface that exhibits a higher surface coverage of **1**. It is important to control the surface coverage of **1** on the sensing interface to an optimal value that leads to superior recognition functions for the analyte DNA. We believe that a surface coverage of **1** on the sensing surface corresponding to ca. 6×10^{-11} mol·cm^{-2} represents the optimal surface architecture for the analysis of **2**. A further important aspect related to the formation of the double-stranded assembly between the sensing interface of **1** and the analyte DNA (**2**) involves the kinetics of hybridization. We have studied the time-dependent frequency changes of the **1**-functionalized Au-quartz crystal upon interaction with the target DNA (**2**), 5×10^{-6} M (see Supporting Information). The frequency decreases for ca. 40 min and then levels off to an equilibrium value. The frequency change within the first 10 min, $\Delta f = -17$ Hz, corresponding to a surface coverage of the ds assembly of 20%, is almost identical to the frequency decrease in the next 30 min ($\Delta f = -38$ Hz after 40 min, corresponding to a surface coverage of ca. 43%). Thus, to achieve reasonable sensitivities in the sensing of **2** and to retain low detection times, the time interval used for the hybridization between the sensing interface and **2** was limited in the further QCM experiments to 10 min. The hybridization process between the sensing interface and **2** can also be followed by Faradaic impedance spectroscopy. While the **1**-functionalized-electrode exhibits, in the presence of $Fe(CN)_6^{3-}/Fe(CN)_6^{4-}$ as redox-label, an interfacial electron-transfer resistance corresponding to $R_{et} = 3.2$ kΩ, the hybridization of the interface with **2** for 10, 30, and 40 min increases the interfacial electron-transfer resistances to 4.5, 5.7, and 6.8 kΩ, respectively. The increase in the interfacial electron-transfer resistances upon hybridization with **2** is attributed to the electrostatic repulsion of the redox label by the charged interface.

Figure 4A shows the Faradaic impedance spectra upon the amplified sensing of **2** by the **3**-functionalized liposomes according to Scheme 1A. While the hybridization of **2** with the interface increases the electron-transfer resistance from 3.2 to 4.1 kΩ, the association of the DNA-tagged liposomes induces a very high increase in the interfacial electron-transfer resistance, $R_{et} = 15.4$ kΩ. That is, the negatively charged liposome micromembrane repels effectively the redox label and introduces a high barrier for the electron-transfer event. This high barrier, induced by the liposomes for interfacial electron transfer, is only observed as a result of a recognition event between **1** and the target DNA (**2**). An identical experiment (see Supporting Information) where the sensing interface was challenged with the noncomplementary DNA (**2a**) and then with the **3**-labeled

(27) No significant changes in the interfacial electron-transfer resistances were observed in the presence of 1,1′-dihydroxymethylferrocene as redox-label. This supports the electrostatic repulsion mechanism of $Fe(CN)_6^{3-/4-}$ by the oligonucleotide monolayer, as the major effect in controlling the interfacial electron-transfer resistances.

(28) (a) Bardea, A.; Katz, E.; Willner, I. *Electroanalysis* **2000**, *12*, 1097−1106. (b) Kharitonov, A. B.; Alfonta, L.; Katz, E.; Willner, I. *J. Electroanal. Chem.* **2000**, *487*, 133−141. (c) Patolsky, F.; Filanovsky, B.; Katz, E.; Willner, I. *J. Phys. Chem. B* **1998**, *102*, 10359−10367.

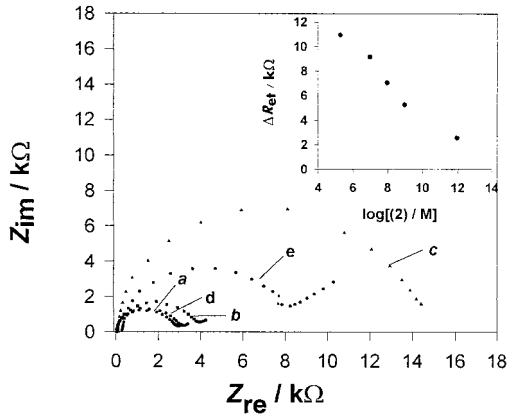

Figure 4. Faradaic impedance spectra (Nyquist plots) of the (a) **1**-functionalized Au electrode, (b) after interaction of the sensing electrode with **2**, 5×10^{-6} M (40 min, 37 °C), (c) after interaction with the **3**-functionalized liposome (lipid concentration 0.2 mM), (d) after hybridization of the sensing interface with **2**, 1×10^{-9} M (40 min, 37 °C), and (e) after treatment of the hybridized interface with the **3**-functionalized liposomes. Inset: Changes in the electron-transfer resistances of the **1**-functionalized electrode upon treatment with different concentrations of the analyte DNA (**2**) and secondary amplification with the **3**-functionalized liposomes. ΔR_{et} corresponds to the difference in the electron-transfer resistance after amplification with the (**3**)-functionalized liposome and the resistance of the **1**-modified electrode. All measurements were performed with Au electrodes (0.2 cm^2, roughness factor 1.2−1.5) in a 0.1 M phosphate buffer, pH 7.2, that included $Fe(CN)_6^{3-/4-}$, 5×10^{-3} M (1:1), at a bias potential of 0.18 V vs SCE, in the frequency range of 100 MHz to 10 kHz, using an alternate voltage, 5 mV.

liposomes revealed only a minute increase in the interfacial electron-transfer resistance, $\Delta R_{et} = 0.3$ kΩ, that is attributed to nonspecific association of the liposomes to the sensing interface. Thus, the amplified detection and analysis of the target DNA by the oligonucleotide-tagged liposomes is specific. The change in the interfacial electron-transfer resistance as a result of the attempt to sense the high concentration, 5×10^{-6} M, of the noncomplementary DNA by the labeled liposomes may be considered as the noise level of the detection method. Figure 4 (inset) shows the calibration curve that corresponds to the changes in the interfacial electron-transfer resistances upon the analysis of different concentrations of the DNA (**2**) according to Scheme 1A (ΔR_{et} is defined as the difference between the electron-transfer resistance of the electrode after the association of the liposomes and the electron-transfer resistance of the **1**-functionalized electrode). Note that the target DNA can be sensed with a sensitivity limit of 1×10^{-12} M (S/N > 5).

Figure 5A shows the microgravimetric, quartz-crystal microbalance (QCM) analysis of the target DNA (**2**) in accordance with Scheme 1A. Interaction of the **1**-functionalized Au-quartz crystal with **2**, 5×10^{-6} M, results in a frequency change of ca. −18 Hz, and interaction with the **3**-functionalized liposomes results in a further frequency change of −100 Hz, Figure 5A curves a and b, respectively. Treatment of the sensing interface with the noncomplementary DNA (**2a**) and then interaction of the resulting interface with the tagged liposomes results in a minute frequency change, ca. −2 Hz, Figure 5A, curves e and f, respectively, indicating that the sensing process is specific. At low concentrations of the analyte DNA, 5×10^{-9} M, the hybridization of **2** with the sensing surface cannot be detected by the piezoelectric crystal. Nonetheless, the association of the high molecular-weight liposomes is easily detected by crystal (Cf. Figure 5, curves c and d). Figure 5B shows the crystal frequency changes as a result of the association of the **3**-functionalized liposomes on the ds assembly resulting in the sensing of different concentrations of **2**. We find that upon the sensing of the target DNA (**2**), in the concentration range of 1×10^{-5} to 1×10^{-8} M, the crystal frequency change as a result of the association of the liposomes is almost similar, $\Delta f = -110$ to −120 Hz. Thus, in this concentration range of the analyte-DNA the sensing interface is saturated with the target DNA. The coverage of the sensing interface by the liposomes is, however, controlled by the concentration of the analyte DNA in the sample for concentrations $< 5 \times 10^{-8}$ M.

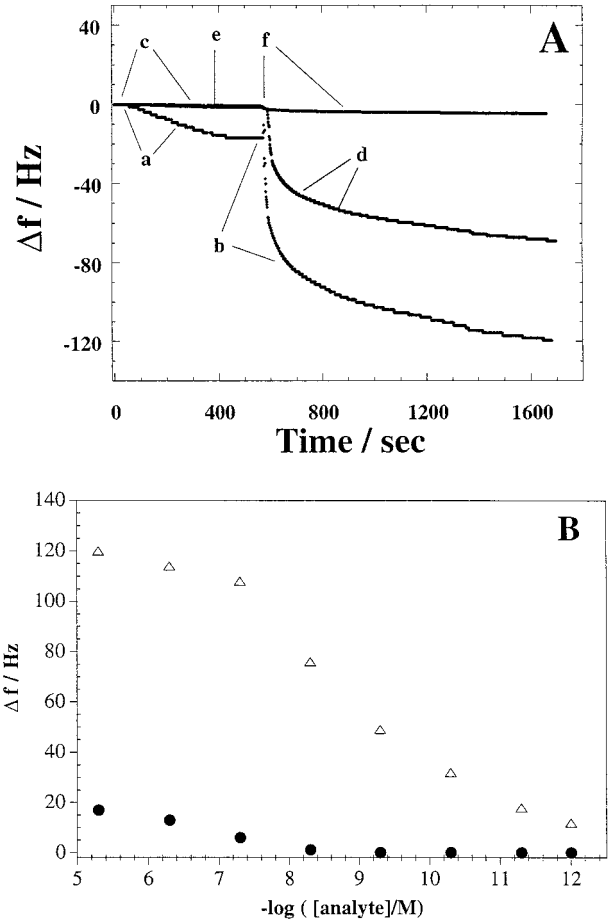

Figure 5. (A) Time-dependent frequency changes of the **1**-functionalized Au-quartz crystal upon (a) interaction with **2**, 5×10^{-6} M, (b) after interaction of the resulting electrode with the **3**-functionalized liposomes (lipid concentration 0.2 mM), (c) treatment of the **1**-functionalized Au-quartz crystal with **2**, 5×10^{-9} M, (d) subsequent treatment of the resulting electrode with the **3**-tagged liposomes (lipid concentration 0.2 mM), (e) treatment of the **1**-functionalized-Au/quartz crystal with **2a**, 5×10^{-6} M, and (f) treatment of the hybridized interface with (**3**)-labeled liposomes. (B) Quartz-crystal frequency changes as a result of (●) interaction of the **1**-modified electrode with different concentrations of the complementary target DNA (**2**) and (△) as a result of the association of the **3**-functionalized liposomes on the ds-assembly resulting from the interaction of the sensing interface with different concentrations of **2**.

The analyte DNA (**2**) was also sensed by the biotin-labeled liposomes according to Scheme 1B. Figure 6A shows the Faradaic impedance spectra of the **1**-functionalized electrode upon the stepwise amplification of the sensing interface with the analyte DNA (**2**) that was pretreated with the biotinylated oligonucleotide, (**4**). The association of the **2**/**4** complex to the sensing layer results in an increase in the interfacial electron-transfer resistance to the value $R_{et} = 5.1$ kΩ, Figure 6A, curve b. The association of the avidin to the surface further increases

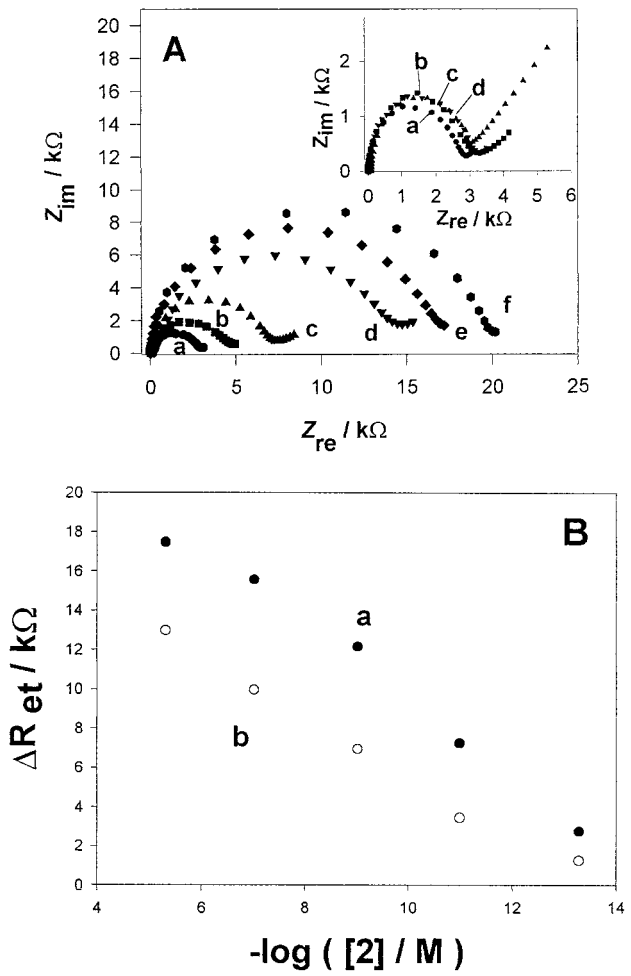

Figure 6. (A) Faradaic impedance spectra (Nyquist plots) of the (a) **1**-functionalized Au electrode, (b) after the interaction of the sensing electrode with **2**, 5×10^{-6} M, pretreated with **4**, 1×10^{-5} M (interaction time 30 min, 37 °C), (c) after treatment of the resulting electrode with avidin, 2.5 μg·mL^{-1}, 15 min, (d) after interaction with the biotinylated liposomes (8 min, lipid concentration 0.25 mM), (e) treatment of the interface for a second time with avidin, 2.5 μg·mL^{-1}, 15 min, and (f) interaction of the interface for a second time with the biotinylated liposomes. All impedance experiments were performed under the conditions detailed in Figure 4. Inset: Faradaic impedance spectra (Nyquist plots) of (a) the **1**-functionalized Au electrode, (b) after interaction of the sensing electrode with **2a**, 5×10^{-6} M, which was pretreated with **4**, 1×10^{-5} M (interaction time 30 min, 37 °C), (c) after treatment of the resulting electrode with avidin, 2.5 μg·mL^{-1}, for 15 min, and (d) after interaction with the biotinylated liposomes (8 min, lipid concentration 0.25 mM). (B) (a) Calibration curve corresponding to the changes in the electron-transfer resistances of the sensing electrode upon interaction with different concentrations of the analyte DNA (**2**) and the enhancement of the sensing processes by a double-step avidin/biotinylated liposomes amplification path. ΔR_{et} corresponds to the difference in the electron-transfer resistance after a double-step avidin/biotinylated liposomes amplification process and the electron-transfer resistance of the **1**-functionalized electrode. (b) Similar calibration curve using a single binding cycle of the biotinylated liposomes.

the electron-transfer resistance to $R_{et} = 7.2$ kΩ, Figure 6A, curve c, and the binding of the biotin-labeled liposome results in a pronounced increase in the interfacial electron-transfer resistance to $R_{et} = 15.5$ kΩ, Figure 6A, curve d. Treatment of the resulting assembly again with avidin and then with the biotinylated liposomes results in the second step of amplification, indicated by the increase of the electron-transfer resistances at the electrode surface to the values $R_{et} = 18$ and 21 kΩ, respectively, Figure 6A, curves e and f. The increase in the electron-transfer resistance at the electrode upon the association of avidin is attributed to the hydrophobic insulation of the electrode that perturbs the interfacial electron transfer. The substantial increase of the electron-transfer resistance upon the association of the biotin-labeled liposomes is attributed to the electrostatic repulsion of the redox label, $Fe(CN)_6^{3-}/Fe(CN)_6^{4-}$, upon the association of the negatively charged liposome micromembranes to the electrode. Figure 6A, inset, shows the Faradaic impedance spectra that corresponds to the control experiment where the sensing interface is interacted with the noncomplementary DNA (**2a**), pretreated with the biotinylated oligonucleotide (**4**), Figure 6A, inset, curve b, and then reacted with avidin and the biotin-tagged liposomes, Figure 6A, inset, curves c and d, respectively. The interfacial electron-transfer resistance in the entire process of sensing the noncomplementary analyte (**2a**) increases only by ca. 0.3 kΩ. This change in the electron-transfer resistance is attributed to nonspecific binding of the different components to the sensing interface, and thus may be considered as the inherent noise level of the measurements. Thus, the association of the avidin/biotinylated liposomes to the sensing interface occurs selectively only upon the primary formation of the three-component ds assembly **1**/**2**/**4**. Binding of the liposomes to the interface amplifies the primary recognition event since the micromembrane assembly generated on the conductive support introduces a pronounced barrier for the electron transfer at the electrode surface. The amount of the three-component ds assembly **1**/**2**/**4** on the electrode is controlled by the concentration of the analyte DNA (**2**) in the sample. As the concentration of **2** decreases, the coverage of the interface is reduced (see Supporting Information). Thus, the coverage of the surface by avidin/biotinylated liposomes and the resulting increase in the electron-transfer resistances are controlled by the concentration of **2**. Figure 6B, curve a, shows the calibration curve that corresponds to the changes in the interfacial electron-transfer resistances, ΔR_{et}, as a result of the double-step association of the avidin/biotinylated liposomes to the sensing interface and the analysis of different concentrations of **2**. Realizing that the noise level of the system is ca. $\Delta R_{et} = 0.9$ kΩ, the target DNA can be analyzed at a sensitivity limit of 1×10^{-13} M (S/N > 3). For comparison, we present the calibration curve corresponding to the amplified analysis of **2** using a single binding cycle of the biotinylated liposomes, Figure 6B, curve b. We realize that at low concentrations of the analyte (**2**), we observe a nonlinear, dendritic-type, amplification of the analysis of **2** by the biotinylated liposomes.

The multistep amplification of DNA sensing by the biotin-labeled liposomes was also probed by microgravimetric quartz-crystal-microbalance measurements. Figure 7A shows the stepwise amplified sensing of **2** by the **1**-functionalized Au-quartz crystal. Hybridization of **2**, prehybridized with **4**, with the interface, Figure 7A, step a, results in a small frequency change of ca. −14 Hz. Association of avidin with the interface, Figure 7A, step b, is accompanied by a frequency decrease of 50 Hz. Binding of the biotin-labeled liposomes, Figure 7A, step c, induces a sharp decrease in the frequency of the crystals that corresponds to ∼500 Hz. By the secondary association of avidin and the tagged liposomes, Figure 7A, steps d and e, respectively, the crystal frequency changes by an additional value corresponding to −800 Hz. When the **1**-functionalized crystal was interacted with the noncomplementary DNA (**2a**), pretreated with **4**, and then reacted with avidin and the biotin-labeled liposomes, Figure 7A, steps f, g, and h, respectively, a minute

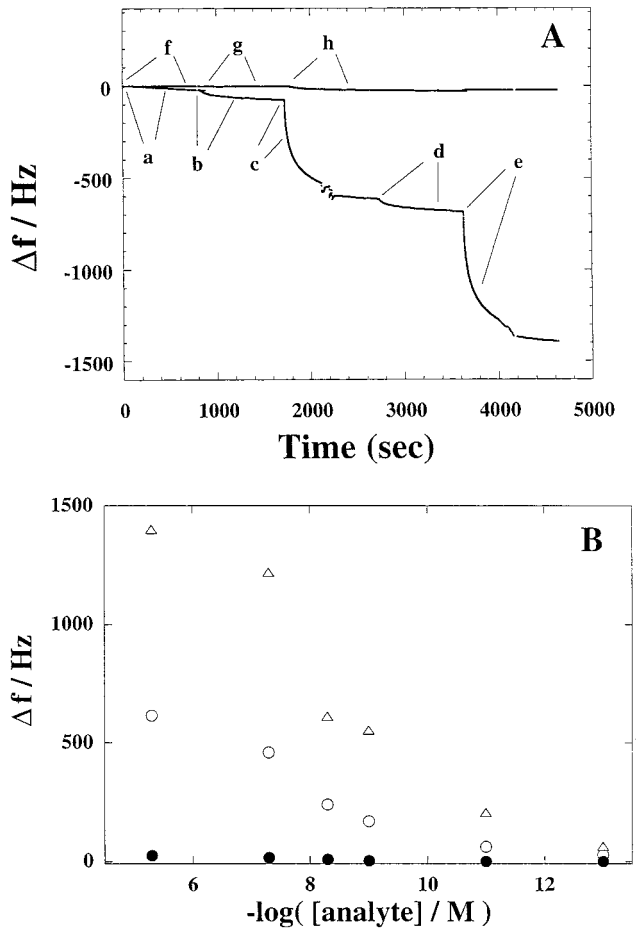

Figure 7. (A) Time-dependent frequency changes of the Au-quartz crystal upon (a) interaction of the sensing interface with **2**, 5×10^{-6} M, and **4** 1×10^{-5} M complex, (b) as a result of the reaction of the resulting interface with avidin, 2.5 μg·mL^{-1}, (c) upon reacting the resulting assembly with the biotin-labeled liposome, (d) step b repeated, (e) step c repeated, (f) treatment of the sensing interface with the **2a**/**4** complex; (g) interaction of the resulting interface with avidin, and (h) reacting the resulting interface with biotin-labeled liposomes (lipid concentration 0.25 mM). (B) Quartz-crystal frequency changes as a result of (●) interaction of the **1**-modified electrode with different concentrations of the target DNA (**2**) and (○) the sensing of different concentrations of the analyte (**2**) upon the one-step amplified detection process with avidin and biotin-labeled liposomes and (△) upon the sensing of variable concentrations of **2** by the two-step amplified detection with biotin-labeled liposomes.

change in the crystal frequency, $\Delta f = -2$ Hz, was observed. This confirms that the sensing of the analyte DNA (**2**) is specific and that the liposomes provide a gravimetric probe for the amplification of the DNA sensing event. Figure 7B shows the frequency changes of **1**-functionalized Au-quartz crystals as a result of the sensing of different concentrations of the analyte (**2**) upon the two-step amplified detection process using the biotin-labeled liposomes. The amplification is nonlinear due to the dendritic pattern of the amplification route. The dendritic-type amplification is specifically illustrated at low concentrations of the target DNA (**2**), $<1 \times 10^{-9}$ M, where the hybridization with the sensing interface leads to a low surface coverage. For example, at analyte concentrations of 1×10^{-8} and 1×10^{-11} M, the first step of amplification with the liposomes results in frequency changes of -190 and -50 Hz, respectively, while in the second amplification cycle with the liposomes, the frequency changes by additional values corresponding to -360 and -150 Hz, respectively.

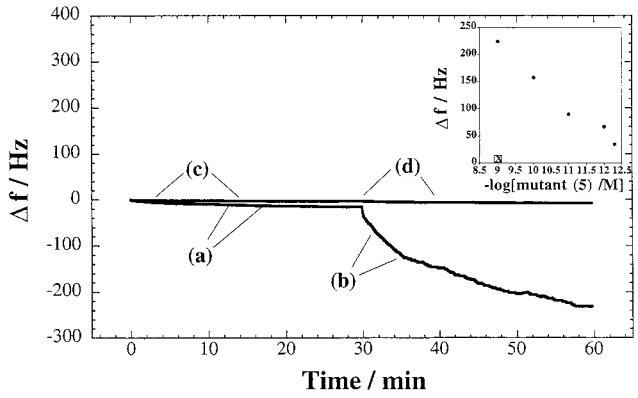

Figure 8. Time-dependent frequency changes and single-base mismatch detection upon the analysis of **5** or **5a** according to Scheme 2. The **6**-functionalized Au-quartz crystals were reacted with **5** or **5a**, 1×10^{-9} M, for 60 min in 2 × SSC, pH 7.5. The resulting electrodes were reacted with biotinylated-dCTP, 20 μM, and polymerase Klenow fragment, 20 U·mL^{-1} in Tris buffer solution, pH =7.5, for 40 min. The resulting electrodes were placed in the QCM cell: (a and c) frequency changes after addition of avidin, 2.5 μg·mL^{-1} and (b and d) frequency changes upon addition of biotin-labeled liposomes (lipid concentration 0.25 mM). (a) and (b) correspond to the analysis of **5**, whereas (c) and (d) correspond to the analysis of **5a**. Measurements in QCM cell were performed in Tris buffer solution, pH 7.5. Inset: Total frequency changes of the **6**-functionalized Au-quartz crystal upon the sensing of different concentrations of the mutant **5**, as outlined in the figure. Point X corresponds to the frequency change observed with the normal gene (**5a**) upon its analysis according to the process outlined in the figure.

The biotin-tagged liposomes were used as an amplifying probe for the identification and sensing of single-base mismatches in an analyte DNA. Scheme 2 outlines the method for the identification of a single G-base mismatch in **5** that substitutes the A-base in the normal gene sequence (**5a**). A primer oligonucleotide (**6**), which is complementary to the target analyte up to one-base before the mutation site, is assembled on the Au electrode. The DNA with the single-base mismatch (**5**), as well as the normal gene (**5a**), hybridizes with the sensing interface. The resulting ds assemblies are then reacted with biotin-labeled-dCTP in the presence of polymerase I (Klenow fragment). The biotinylated dCTP couples to the double-stranded assembly that includes the mutant (**5**), but the base will not couple to the double-stranded system that includes the normal gene (**5a**). Treatment of the resulting assemblies with avidin, and then with the biotin-labeled liposomes, will result in the association of the liposomes to the double-stranded assembly that includes the single-base mismatch and the coupled biotinylated-C. Note that the liposome will only bind to the assembly that includes the analyte with the single-base (G) mismatch.

The binding of the liposomes to the sensing interface may be detected by microgravimetric quartz-crystal-microbalance analyses or Faradaic impedance measurements. Figure 8 shows the frequency changes of Au/quartz crystals that analyze the mutant (**5**) and the normal gene (**5a**), according to Scheme 2. The Au/quartz crystals were functionalized with **6**, surface coverage 2.3×10^{-11} mol·cm^{-2}, and then interacted with **5** or **5a**, respectively. The resulting assemblies were then reacted with biotinylated-dCTP and polymerase. Figure 8, curve a, shows the crystal frequency change upon treatment of the resulting ds assembly that includes the mutant (**5**) after the biotinylated base insertion with avidin. The crystal frequency decreases by ca. -20 Hz, indicating the association of avidin to the interface. Addition of the biotinylated liposomes to the resulting system leads to the time-dependent frequency decrease of the crystal

shown in Figure 8, curve b. The crystal frequency decreases by ca. 230 Hz, indicating that the "heavy" liposomes bind to the surface. The control experiment, where the double-stranded assembly that includes the normal gene (**5a**) treated with dCTP/polymerase, and interacted with avidin and then the biotin-tagged-liposomes, is depicted in Figure 8, curves c and d, respectively. The crystal frequency does not change, indicating that the biotin-tagged liposomes do not bind to the interface that includes the normal gene (**5a**). Thus, the biotinylated liposome binds specifically to the double-stranded assembly where the biotinylated C-base was coupled by the polymerase-induced reaction.

Figure 8 (inset) shows the frequency changes of the Au-quartz crystal upon the analysis of different concentrations of the mutant (**5**) by its association to the sensing interface followed by the polymerase-induced coupling of biotinylated dCTP and then the assay of the resulting assembly with avidin and the biotin-labeled liposomes. As the concentration of the mutant in the sample decreases, the amount of associated DNA with the sensing interface is lower, and the frequency changes resulting from the association of the liposomes are lower in their magnitudes. The point X in Figure 8 (inset) corresponds to the analysis of the normal gene (**5a**), 1×10^{-9} M, by the **6**-functionalized Au-quartz crystal using the sequence outlined in Scheme 2, followed by an attempt to bind the biotinylated liposomes to the interface. A frequency decrease corresponding to less than 5 Hz is observed, and this is attributed to the nonspecific adsorption of the liposomes to the interface. Note, however, that at a mutant **5** concentration of 5×10^{-13} M the frequency change as a result of the association of the liposomes is ca. -35 Hz. Thus, the mutant at a concentration of 5×10^{-13} M can be effectively differentiated from the normal gene, 1×10^{-9} M (S/N > 7).

The detection of the single base mismatch in the mutant (**5**), using the polymerase-induced coupling of biotinylated-dCTP and the association of the tagged liposomes, can also be transduced by Faradaic impedance measurements. Figure 9A shows the Faradaic impedance spectra upon the amplified detection of the mutant (**5**). The **6**-functionalized electrode, Figure 9A, curve a, exhibits an interfacial electron-transfer resistance of 1.8 kΩ. The hybridization of the mutant (**5**) with the sensing interface slightly increases the interfacial electron-transfer resistance due to the electrostatic repulsion of the $Fe(CN)_6^{3-/4-}$ redox label by the ds assembly on the electrode support. The polymerase-induced coupling of the biotinylated C-base to the assembly does not alter significantly the interfacial electron-transfer resistance, Figure 9A, curve c. The binding of avidin, Figure 9A, curve d, and then the association of the liposomes, Figure 9A, curve e, substantially increase the interfacial electron-transfer resistance to the values $R_{et} = 6.8$ and 14.0 kΩ, respectively. The increase in the interfacial electron-transfer resistances upon the binding of avidin and the association of the liposomes is attributed to the hydrophobic insulation of the electrode by the protein and to the electrostatic repulsion of the redox-label $Fe(CN)_6^{3-/4-}$ by the negatively charged liposomes, respectively. Figure 9B depicts the calibration curve that corresponds to the difference in the electron-transfer resistances ΔR_{et} upon the sensing of the different concentrations of the mutant (**5**) by the biotinylated liposomes (ΔR_{et} corresponds to the difference between the electron-transfer resistance of the electrode after the binding of the liposomes and the electron-transfer resistance of the **6**-functionalized electrode after hybridization with **5**). Point "Y" in Figure 9B indicates the ΔR_{et} value of the **6**-functionalized electrode after

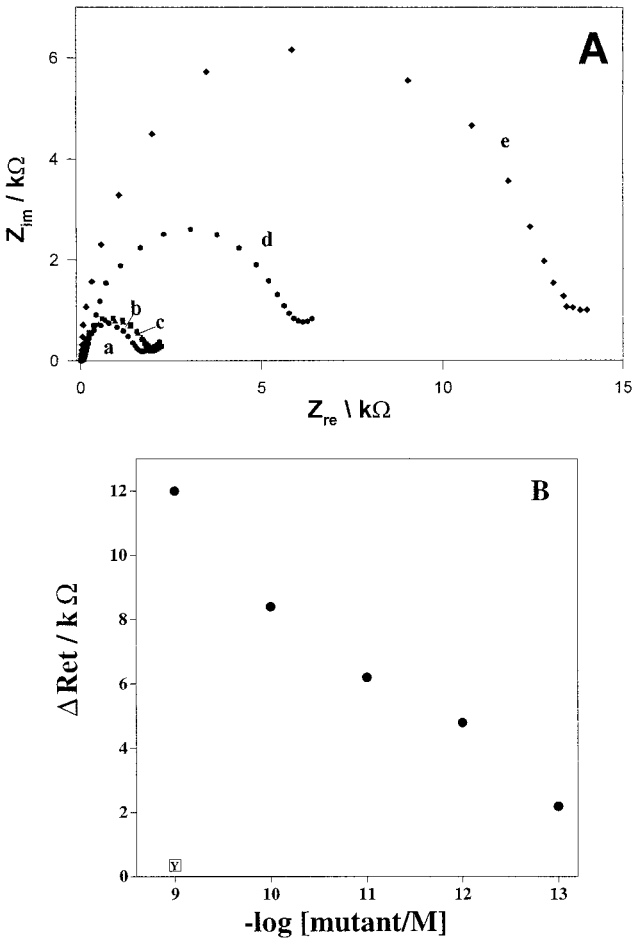

Figure 9. (A) Faradaic impedance spectra (Z_{im} vs Z_{re}) upon the analysis of the single-base mismatch in **5**: (a) the **6**-functionalized electrodes, (b) the **6**-functionalized electrode after hybridization with **5**, 1×10^{-9} M, for 60 min in 2 × SSC buffer, pH 7.5, 37 °C, (c) after reaction of the double stranded interface with biotinylated-dCTP, 20μM, and polymerase Klenow fragment, 20 U·mL^{-1} for 40 min, (d) after the interaction of the electrode with avidin, 2.5 μg·mL^{-1}, and (e) after the interaction of the interface with the biotinylated liposomes (lipid concentration 0.25 mM), 20 min. (B) Correlation between ΔR_{et} observed upon the sensing of different concentrations of the mutant **5** according to the process outlined in part A. ΔR_{et} corresponds to the difference between the electron-transfer resistance at the electrode after the binding of the biotinylated liposomes and the electron-transfer resistance of the **6**-functionalized electrode after hybridization with **5**.

the analysis of the normal gene (**5a**) by the biotinylated liposomes according to Scheme 2. The slight increase in the interfacial electron-transfer resistance, $\Delta R_{et} \approx 0.34$ kΩ, is attributed to the nonspecific association of the liposomes to the interface. Note that the mutant (**5**) at a concentration of 1×10^{-13} M ($\Delta R_{et} = 2.0$ kΩ) can be easily differentiated from the normal gene (**5a**) at a concentration of 1×10^{-9} M, $\Delta R_{et} = 0.34$ kΩ (S/N ≥ 6).

Conclusions

The present study has addressed a novel method to amplify oligonucleotide-DNA binding interactions, or single base mismatches, by the use of functionalized liposomes. The selective association of the liposomes to the interface that includes the target DNA generates a micromembrane assembly that alters the physicochemical interfacial properties of the respective electronic transducers. The deposition of negatively charged liposomes on electrode supports results in a charged interface

that repels negatively charged redox labels. This introduces an electron-transfer barrier (resistance) for the electron transfer between the electrode and $Fe(CN)_6^{3-}/Fe(CN)_6^{4-}$, thus enabling the electronic transduction of the DNA sensing by Faradaic impedance spectroscopy. Similarly, the association of the liposomes onto the Au-quartz crystals enables the microgravimetric, quartz-crystal-microbalance (QCM) transduction of the DNA sensing processes. The results reveal very sensitive and specific DNA sensing in the presence of these amplifying probes. The use of tagged liposomes for probing DNA interactions provides a model for the application of other nanocomposites such as particles or clusters for DNA analyses. The functionalized liposomes provide a building block for the construction of dendritic assemblies upon sensing of DNA, and thus provide a novel approach for the amplified analysis of DNA and the detection of single-base mismatches. An important advantage for using liposomes in the amplified DNA sensing is the fact that the liposome may act as a "nanocontainer" for additional components that may stimulate secondary amplification processes. The incorporation of fluorescence labels, enzymes, bioluminescent units, etc. into the interior aqueous compartments of the liposomes, or into the hydrophobic bilayer, may lead to such amplification routes.

Acknowledgment. Parts of this research are supported by an EC ATOMS grant and by the Israel Ministry of Science as a part of an Israel−Japan Cooperation program.

Supporting Information Available: Experimental details for the preparation of the anionic liposomes are described; the analysis of the kinetics of hybridization of **2** with the **1**-functionalized interface is provided; the analysis of mutant **2a** by the sensing interface with **3**-functionalized liposomes and Faradaic impedance spectroscopy as transduction means is given; and the time-dependent frequency changes of the **1**-functionalized Au-quartz crystal upon hybridization with different concentrations of **2**, pretreated with **4** are presented (PDF). This material is available free of charge via the Internet at http://pubs.acs.org.

JA0036256